



An electrochemical analysis of AZ91 Mg alloy processed by plasma electrolytic oxidation followed by static annealing

Y.G. Ko^a, K.M. Lee^b, B.U. Lee^b, D.H. Shin^{b,*}

^a School of Materials Science and Engineering, Yeungnam University, 214-1 Dae-Dong, Gyeongsan 712-749, Gyeongbuk, South Korea

^b Department of Metallurgy and Materials Engineering, Hanyang University, Ansan 425-791, South Korea

ARTICLE INFO

Article history:

Received 12 July 2010

Received in revised form 15 October 2010

Accepted 7 December 2010

Available online 14 December 2010

Keywords:

Plasma electrolytic oxidation

AZ91 Mg alloy

Static annealing

Electrochemical analysis

ABSTRACT

In this study, the effect of subsequent annealing on the electrochemical response of AZ91 Mg alloy coated via plasma electrolytic oxidation (PEO) was investigated. PEO coating was carried out on the Mg alloy under AC condition in an alkaline silicate electrolyte, and the PEO-coated samples underwent several subsequent annealing treatments at three different temperatures of 100, 150, and 200 °C. The surface morphologies of the coating layers were observed via a scanning electron microscope (SEM) and their constituent compounds were characterized by qualitative observation based on X-ray photoelectron spectroscopy (XPS). In addition, the corrosion protection properties of the PEO-coated sample were examined by electrochemical impedance spectroscopy (EIS) in a 3.5 wt% NaCl solution with a focus on exploring the effect of subsequent annealing on the electrochemical response in a quantitative manner. SEM and XPS observations evidenced that the subsequent annealing at temperatures higher than 150 °C resulted in significant morphological changes due to the dehydration reaction of Mg(OH)₂ to form MgO. Thus, it was found that the sample annealed at 150 °C exhibited a better corrosion resistance than the other samples, which were analyzed by taking an equivalent circuit model into account.

© 2011 Elsevier B.V. All rights reserved.

1. Introduction

In recent years, much attention has long been paid to development of Mg alloys since they could be used in a variety of automobile applications where reduction in weight was most required owing to good material properties such as low density and good specific strength [1–3]. Unfortunately, there has been a strong limitation arising from weak corrosion protection of the passive films when Mg alloys were utilized in actual conditions, particularly corrosive environment [4,5]. Protection of Mg alloys from external corrosion was of great importance. To this end, several traditional coating methods such as electrochemical plating and anodizing have been applied to form coating films in order to improve corrosion resistance [6,7]. But, earlier work showed that the adhesive strength between substrate and ceramic films were not always strong [8]. Thus, plasma electrolytic oxidation (PEO) technique has been studied since the electrochemical reaction would result in a better adhesion between substrate and coating layer by applying an extremely high dielectric discharge in a suitable electrolyte [9–11].

In general, the oxide film on Mg alloys via PEO process was known to consist of the outer layer and the inner layer close to

the substrate [12]. The outer layer was relatively thicker than the inner layer, but the outer layer might be weak against corrosion attack due to many pores. In order to improve corrosion protection, the modification of the outer layer was required with respect to the constituent compounds being existed. The major compounds in the oxide film of Mg alloys were Mg(OH)₂ and MgO. The increasing MgO/Mg(OH)₂ ratio in the oxide film would improve the corrosion properties since the quasi-passive Mg(OH)₂ showed poorer corrosion resistance than MgO [13]. Hsiao et al. [14] reported that the MgO/Mg(OH)₂ ratio was increased by the dehydration of Mg(OH)₂ during static annealing and corrosion properties were considerably enhanced. To present, however, the role of each oxide layer on corrosion resistance of the annealed Mg alloys has been rarely discussed. In the present research, the main purpose is two-fold. First is to investigate the influence of annealing treatment on PEO-coated AZ91 Mg alloy. Based on these results, the corrosion response of the present samples was analyzed quantitatively in relation to the optimized equivalent circuit model.

2. Experimental procedures

The chemical composition of the AZ91 Mg alloy used in this study was analyzed as Mg–8.29Al–0.83Zn–0.31Mn in wt%. A 2-mm thick plate was cut into 30 mm × 50 mm samples, which were polished with #1000 SiC paper, rinsed with distilled water, and ultrasonically cleaned in ethanol. The PEO process was carried out in the electrolyte consisting of 0.18 M KOH + 0.09 M KF + 0.08 M Na₂SiO₃. The applied current density was held at 25 mA/cm² for 150 s. After the PEO pro-

* Corresponding author. Tel.: +82 31 400 5224; fax: +82 31 417 3701.
E-mail address: dhshin@hanyang.ac.kr (D.H. Shin).

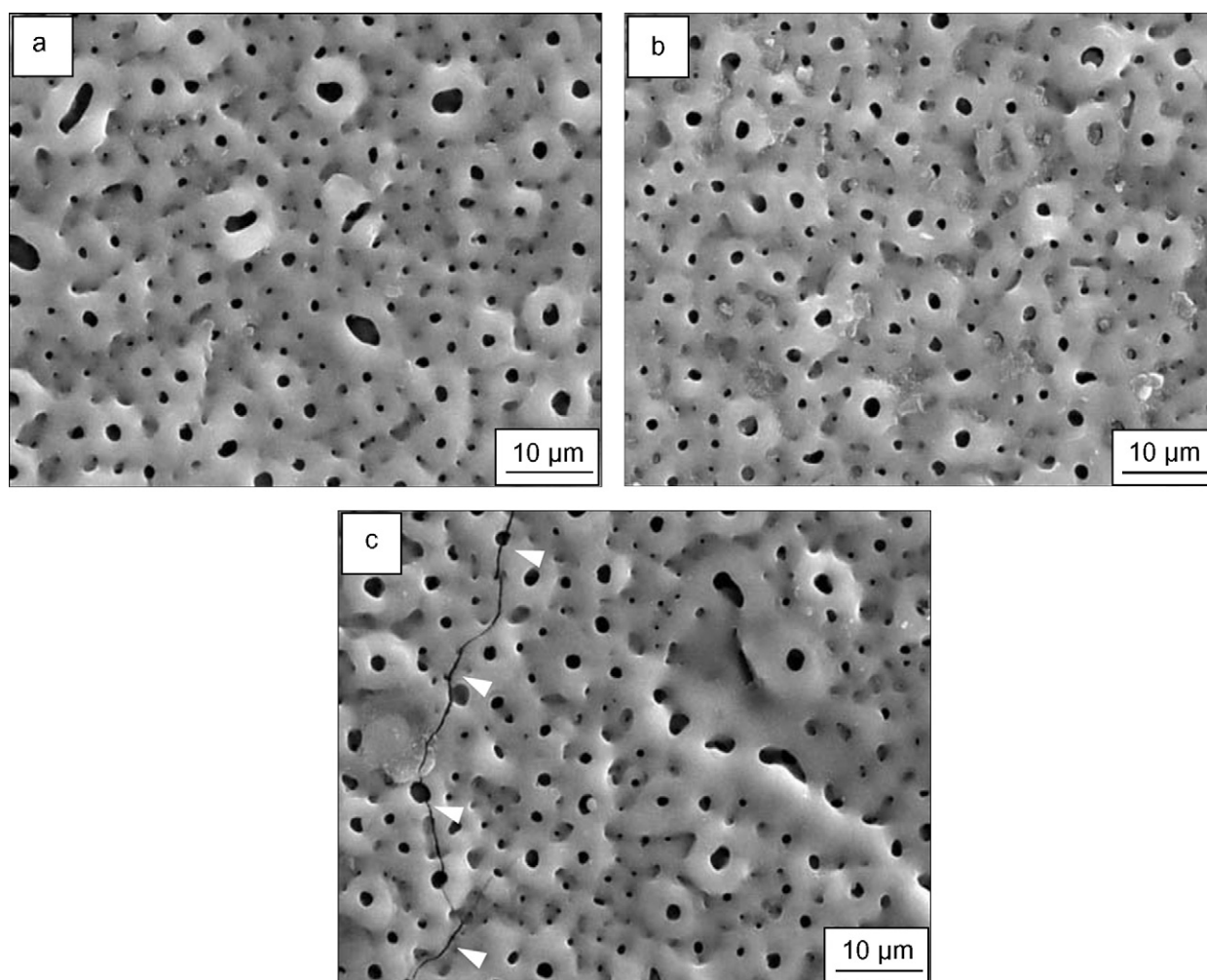


Fig. 1. Surface morphologies of the oxide films annealed at three different annealing temperatures of (a) 100 °C, (b) 150 °C, and (c) 200 °C, respectively.

cess, all samples were annealed at 100, 150, and 200 °C for 10 h in high purity Ar gas.

The surface morphologies of the oxide films were observed via a scanning electron microscope (SEM). For chemical analysis, surface chemistry was analyzed by X-ray photoelectron spectroscopy (XPS) with a monochromatic Al K α source. The electron take-off angle was fixed at 45° and the vacuum pressure was less than 10⁻⁹ Torr during the data acquisition process. Potentiodynamic polarization and electrochemical impedance tests were utilized to evaluate the corrosion resistance of the oxide film using a Reference 600 potentiostat (Gamry Instruments, Warminster, PA, USA) with Gamry Framework program. These tests were conducted in a glass-vessel container with 3.5% NaCl solution at pH 7.0 equipped with the three electrodes: a coated sample having the exposed areas of 1 cm² as a working electrode, a platinum mesh (20 mm × 20 mm) as a counter electrode and Ag/AgCl electrode as a reference electrode. After 30 min of initial delay, the potentiodynamic polarization curves were measured from -0.25 to 0.4 V with respect to the open circuit potential at a scan rate of 1 mV/s. The electrochemical impedance spectroscopy (EIS) test was gauged from 10⁶ to 0.1 Hz at an interval of 10 points/decade with a 10 mV rms.

3. Results and discussion

The surface morphologies of the PEO-coated AZ91 Mg alloy samples, which were additionally annealed at three different temperatures, are shown in Fig. 1. Regardless of annealing temperature, all samples showed crater-like microstructure with some round shrinkage pores. However, the surface of the sample annealed at 200 °C exhibited significant cracks. It was found that the formation of surface cracks of the PEO-coated sample following annealing

treatment at 200 °C was caused by the shrinkage of the oxide film due to the dehydration reaction [15].

According to the XPS patterns (Mg 2p 3/2) of the PEO-treated samples, which were annealed at three different temperatures shown in Fig. 2, the chemical phases were analyzed. De-convolution analysis of the XPS spectra showed that the binding energy of 49.6 eV corresponded to Mg(OH)₂ while the binding energy of 50.4 eV indicated the existence of MgO. The peak intensity of MgO increased with increasing annealing temperature due to the dehydration of Mg(OH)₂ to form MgO. This finding suggested that the MgO/Mg(OH)₂ ratio was expected to increase as annealing temperature increased.

Corrosion resistance of the PEO-coated samples, which were annealed at three different annealing temperatures, was evaluated by electrochemical potentiodynamic polarization tests in a 3.5 wt% NaCl solution as shown in Fig. 3. The corrosion potential (E_{corr}), the corrosion current density (i_{corr}), the anodic and cathodic Tafel slopes (β_a and β_c , respectively) were obtained from potentiodynamic polarization curves. Using the Tafel least-squares fitting method, β_a , β_c , E_{corr} , and i_{corr} were determined, and the polarization resistance (R_p) values were calculated based on the Stern-Geary equation [16],

$$R_p = \frac{\beta_a \times \beta_c}{2.303 i_{corr} (\beta_a + \beta_c)} \quad (1)$$

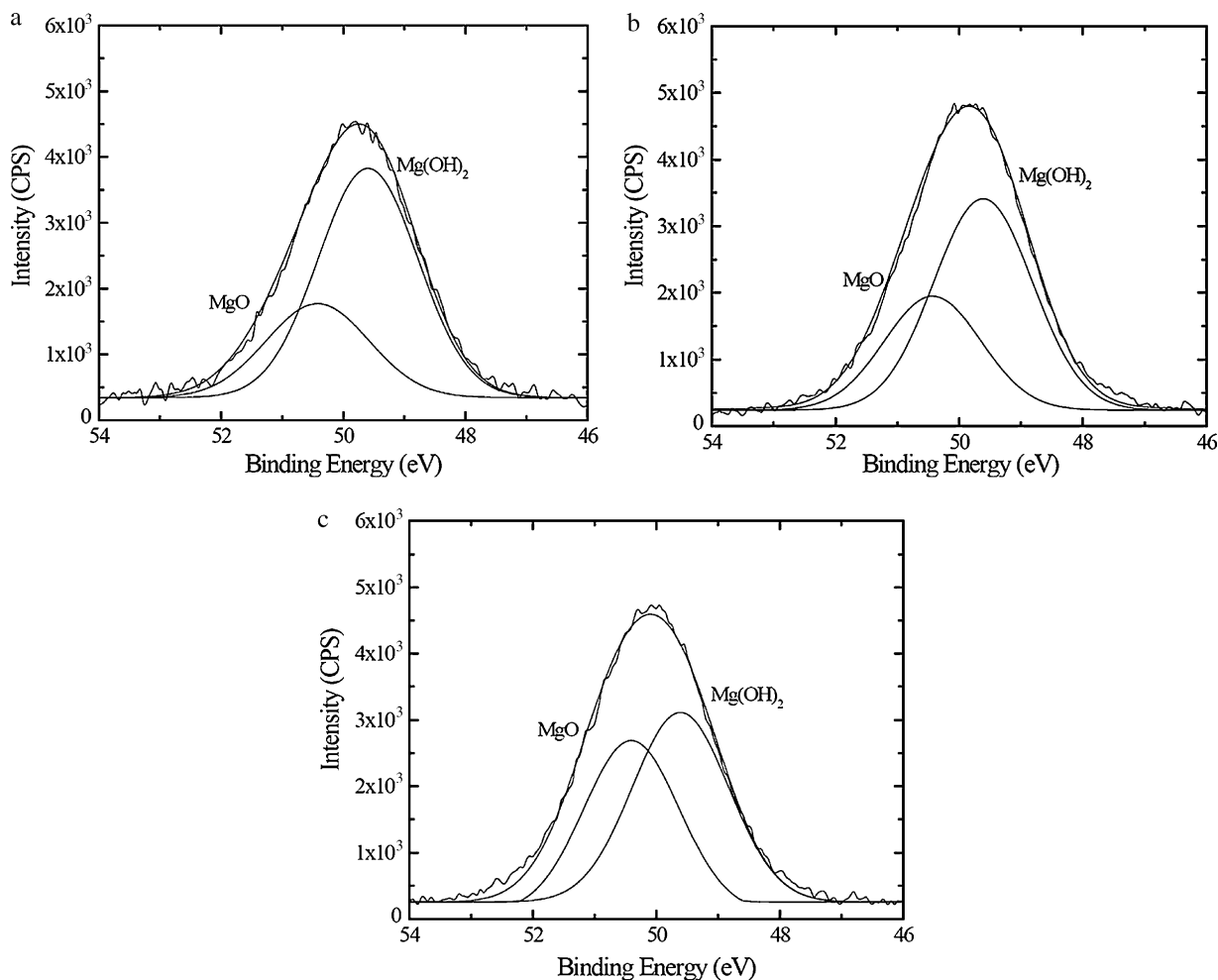


Fig. 2. XPS data of the oxide films annealed at three different annealing temperatures of (a) 100 °C, (b) 150 °C, and (c) 200 °C, respectively.

The results are listed in Table 1. The sample annealed at 150 °C possessed the polarization resistance value of $1.48 \times 10^6 \Omega \text{ cm}^2$. In case of the sample annealed at 200 °C, the polarization resistance was $4.61 \times 10^5 \Omega \text{ cm}^2$ which was similar to that of the sample

annealed at 100 °C. Even if MgO showed a better corrosion resistance than Mg(OH)_2 , the polarization resistance of the sample annealed at 150 °C was the highest among the conditions used in this study since the sample annealed at 200 °C contained surface cracks by volume expansion associated with the transformation of Mg(OH)_2 into MgO.

The electrochemical impedance characteristics of the PEO-treated samples, which were annealed at three different annealing temperatures, are examined in a 3.5 wt% NaCl solution using an open-circuit potential, and related results are displayed in Fig. 4. The Bode and Nyquist plots would shed light on electrochemical behavior of the coating layers. As shown in Fig. 4, the overall tendency of the Bode plots was consistent with that of the Nyquist plots in that the annealing temperature of 150 °C resulted in higher corrosion properties compared to the others. This result was in a good agreement with the surface structure and the relative ratio of $\text{MgO}/\text{Mg(OH)}_2$.

In order to analyze the impedance data in a quantitative manner, the rheological model of equivalent circuit shown in Fig. 5 was used.

Table 1
Results of potentiodynamic polarization tests of the PEO-treated AZ91 Mg alloy samples with respect to annealing temperature.

Annealing temp. (°C)	E_{corr} (V)	i_{corr} (A/cm^2)	β_a (V)	β_c (V)	R_p ($\Omega \text{ cm}^2$)
100	-1.32	3.45×10^{-8}	0.075	0.074	4.69×10^5
150	-1.15	9.61×10^{-9}	0.043	0.135	1.48×10^6
200	-1.22	3.96×10^{-8}	0.077	0.092	4.61×10^5

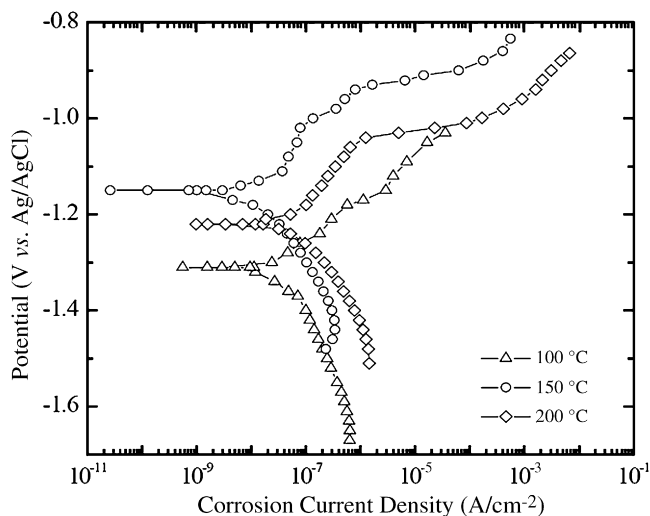


Fig. 3. Potentiodynamic polarization curves of the oxide films annealed at three different annealing temperatures. The potentiodynamic polarization curves were measured from -0.25 to 0.4V with respect to the open circuit potential at a scan rate of 1 mV/s.

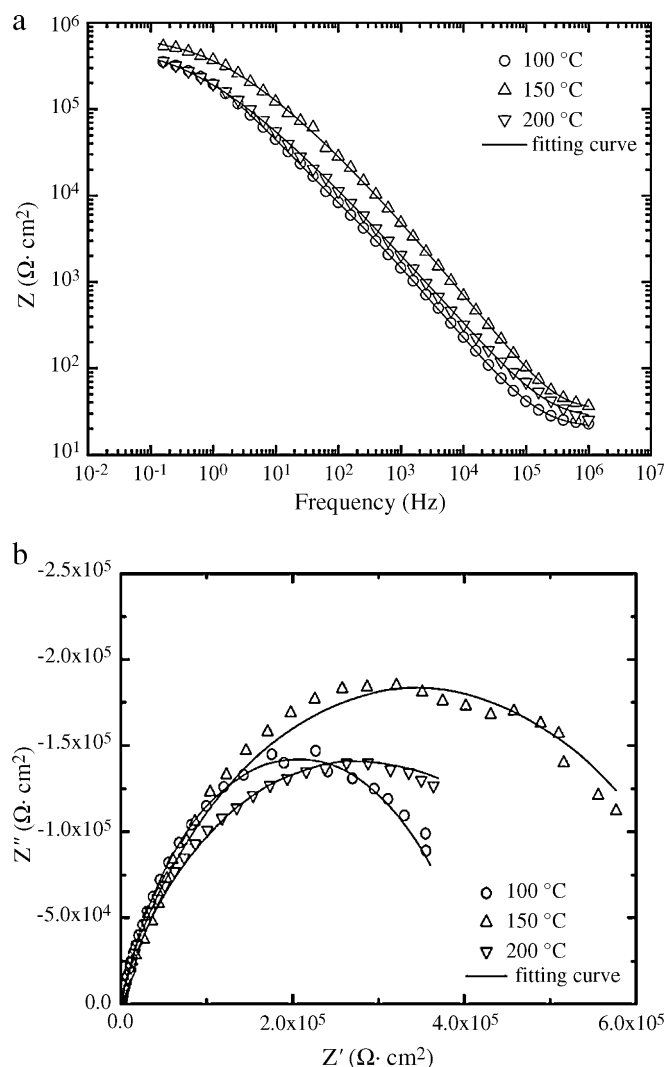


Fig. 4. Electrochemical analysis results of the oxide films annealed at three different annealing temperatures: (a) Bode plots and (b) Nyquist plots.

Within the framework of the equivalent circuit model, the solution resistance (R_s) in a 3.5 wt% NaCl was in series with the unit of the oxide film system. R_o was the outer layer resistance in parallel with the constant phase element (CPE_o). The corrosion properties of the inner layer were described by the resistance R_i that was in parallel with CPE_i . To consider a surface inhomogeneity factor, a more general CPE related to the capacitance dispersion around a mean value was used instead of a rigid capacitive element [17]. The capacity

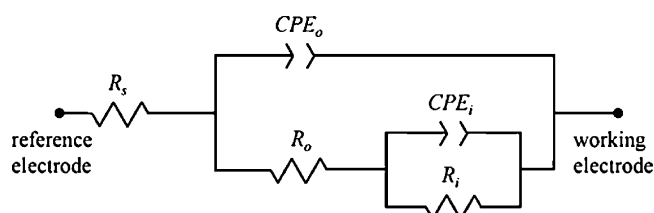


Fig. 5. Rheological model of equivalent circuit consisting of the inner and outer layers working as either resistor or condenser, and solution resistor within an electrical cell. R_s , a solution resistance; R_o , a resistance of an outer layer; R_i , a resistance of an inner layer; CPE_o , a constant phase element meaning an outer layer; CPE_i , a constant phase element meaning an inner layer.

Table 2

Equivalent circuit analysis for the PEO-treated AZ91 Mg alloy samples with respect to annealing temperature. The impedances of the two constant phase elements are defined by a dimensionless n parameter. Subscripts i and o stand for inner and outer layers, respectively. R_s , R_o , and R_i are defined as the resistance of the solution, outer layer, and inner layer, respectively.

Annealing temp. (°C)	R_s (Ω cm ²)	R_o (Ω cm ²)	R_i (Ω cm ²)	$CPE_o - n$	$CPE_i - n$
100	20.23	1.88×10^4	3.98×10^5	0.84	0.60
150	22.38	5.75×10^5	9.23×10^5	0.85	0.55
200	21.70	7.39×10^4	5.14×10^5	0.81	0.45

element was expressed by the following equation;

$$Z_{CPE} = \frac{1}{T(j \times w)^n} \quad (2)$$

where T is the modulus of admittance, j is the imaginary unit, w is the perturbing frequency considered as $w = 2\pi f$, f is the frequency in Hz. The values of n ranged between 0 and 1. For $n=0$, a CPE was a pure resistor, while for $n=1$, a CPE represented a perfect capacitor. Also in case of $n=0.5$, a CPE represented a Warburg diffusion element, which was shown in a Nyquist plot as a straight line with an inclination of 45°. Based on the equivalent circuit model in Fig. 5, the plots were fitted by iteration method using the Echem Analyst program, and the fitting result is shown in Fig. 4 as solid lines passing through the experimental results. A good agreement was observed between the experimental curve and that modeled by the equivalent circuit. The corresponding values of the equivalent elements are listed in Table 2. The resistances (R_o and R_i) of the PEO-coated sample annealed at 150 °C was the highest, implying that corrosion resistance was enhanced. However, they decreased as the annealing temperature continued to rise up to 200 °C, which might be related to a change in the surface structure of the oxide film as seen from Fig. 1c. It was concluded that the annealing temperature of 150 °C would be desirable for PEO-treated AZ91 Mg alloy satisfying corrosion properties.

4. Conclusions

The effect of the annealing treatment on the surface structure and corrosion characteristic of the PEO-treated AZ91 Mg alloy was discussed. Due to the dehydration of $Mg(OH)_2$, the amount of MgO content in the oxide film increased with increasing annealing temperature. However, the corrosion resistance became deteriorated above a temperature of 150 °C because significant cracks appeared due to the volume change arising from the dehydration of $Mg(OH)_2$ to form MgO. Consequently, the corrosion resistance of the oxide film annealed at 150 °C was higher than that of the oxide films annealed at different temperatures. This observation was in line with the analysis based on equivalent circuit model.

Acknowledgements

This work was supported by the National Research Foundation of Korea (2009-0079807). Dr. Y.G. Ko was also grateful for the Yeungnam University research grants in 2009 (209-A-054-028).

References

- [1] R. Nandan, T. DebRoy, H.K.D.H. Bhadeshia, Prog. Mater. Sci. 53 (2008) 980–1023.
- [2] B.L. Mordike, T. Ebert, Mater. Sci. Eng. A 302 (2001) 37–45.
- [3] J.E. Gray, B. Luan, J. Alloys Compd. 336 (2002) 88–113.
- [4] G.L. Song, A. Atrens, Adv. Eng. Mater. 1 (1999) 11–33.
- [5] N.J. Park, J.H. Hwang, J.S. Roh, J. Kor. Inst. Met. Mater. 47 (2009) 1–6.
- [6] Y.W. Song, D.Y. Shan, E.H. Han, Electrochim. Acta 53 (2008) 2135–2143.

- [7] O. Khaselev, D. Weiss, J. Yahalom, J. Electrochem. Soc. 146 (1999) 1757–1761.
- [8] B. Rajasekaran, S.G.S. Raman, L.R. Krishna, S.V. Joshi, G. Sundararajan, Surf. Coat. Technol. 202 (2008) 1462–1469.
- [9] A.L. Yerokhin, X. Nie, A. Leyland, A. Matthews, S.J. Dowey, Surf. Coat. Technol. 122 (1999) 73–93.
- [10] Y.G. Ko, K.M. Lee, K.R. Shin, D.H. Shin, Kor. J. Met. Mater. 48 (2010) 724–729.
- [11] H. Luo, Q. Cai, B. Wei, B. Yu, J. He, D. Li, J. Alloys Compd. 474 (2009) 551–556.
- [12] S.Y. Chang, D.H. Lee, B.S. Kim, T.S. Kim, Y.S. Song, S.H. Kim, C.B. Lee, Met. Mater. Int. 15 (2009) 759–764.
- [13] W. Ximei, Z. Liqun, L. Huicong, L. Weiping, Surf. Coat. Technol. 202 (2008) 4210–4217.
- [14] H.Y. Hsiao, P. Chung, W.T. Tsai, Corros. Sci. 49 (2007) 781–793.
- [15] A.K. Sharma, R.U. Rani, M. Mayanna, Thermochim. Acta 376 (2001) 67–75.
- [16] M. Stern, A.L. Geary, J. Electrochem. Soc. 104 (1957) 56–63.
- [17] A. Ghasemi, V.S. Raja, C. Blawert, W. Dietzel, K.U. Kainer, Surf. Coat. Technol. 202 (2008) 3513–3518.